A.D. 15375

APPLIED PHYSICS LABORATORY

UNIVERSITY OF WASHINGTON

A Division of the Department of Physics

A SEARCH FOR ANOMALOUS ABSORPTION OF HIGH ENERGY NEGATIVE PARTICLES

By W. R. Davis*, G. R. Garrison, J. E. Henderson, C. E. Miller, W. M. Sandstrom

TECHNICAL REPORT

OFFICE OF NAVY RESEARCH

CONTRACT N8onr 52008

Acknowledgment is made to the Bureau of Ordnance, Navy Department for support of the early stages of this research under Contract NOrd 7818.

Approved

J. E. Henderson

J. E. Henderson, Director
Applied Physics Laboratory

*The physical material of this report was presented by W. R. Davis, as a dissertation in partial fulfillment of the requirements for the Degree of Doctor of Philosophy of the Graduate School of the University of Washington.

TABLE OF CONTENTS

LIST OF TABLES

PLATE

LIST OF FIGURES

A SEARCH FOR ANOMALOUS ABSORPTION OF NEGATIVE COSMIC RAY PARTICLES AT SEA LEVEL

CHAPTER I

INTRODUCTION

In previous experiments by this laboratory the large difference between the range-momentum relationships of mu mesons and protons has been used to determine the intensity of cosmic ray protons in the presence of a large background of mu mesons. In these experiments the momentum and sign of the charge of those particles which stopped in a lead absorber were determined by means of a counter-controlled cloud chamber operated in a magnetic field. The experimental arrangements were similar to that shown in Figure II, page 9. The cloud chamber was expanded by those events in which the single Geiger tubes (C_1 and C_2) above and below the chamber were discharged in coincidence while no Geiger tube below the absorber was discharged. In this way, cloud chamber photographs were obtained of those particles which passed through the Geiger counter telescope C_1 and C_2 but failed to traverse the absorber below the chamber.

As an example of the data obtained by this method, the momentum spectra obtained by Garrison at an altitude of 3.4 km for those particles traversing 3.7 g/cm^2 but failing to traverse 223 g/cm^2 of lead equivalent is shown in Figure I. The spectra for positive and negative particles are plotted separately, the difference between the two curves being primarily due to the inclusion of protons among the positive particles. The heavy bars marked "mesons" and "protons" at the base of the graph indicate the momentum intervals for these particles which correspond to the range interval 3.7-223 g/cm^2 of lead equivalent under the assumption that energy loss is due to ionization alone. The spectrum for negative particles is strongly grouped in the momentum interval predicted for mu mesons. The spectrum for positive particles shows two maxima, one in the momentum interval for mu mesons and the other in the interval corresponding to protons. Those protons with momenta less than about 1.1 bev/c are stopped in the lead either by ionization loss or by catastrophic nuclear collisions. Those protons with momenta greater than 1.1 bev/c, and therefore with ionization ranges greater than the thickness of the absorber, are stopped only if they undergo catastrophic

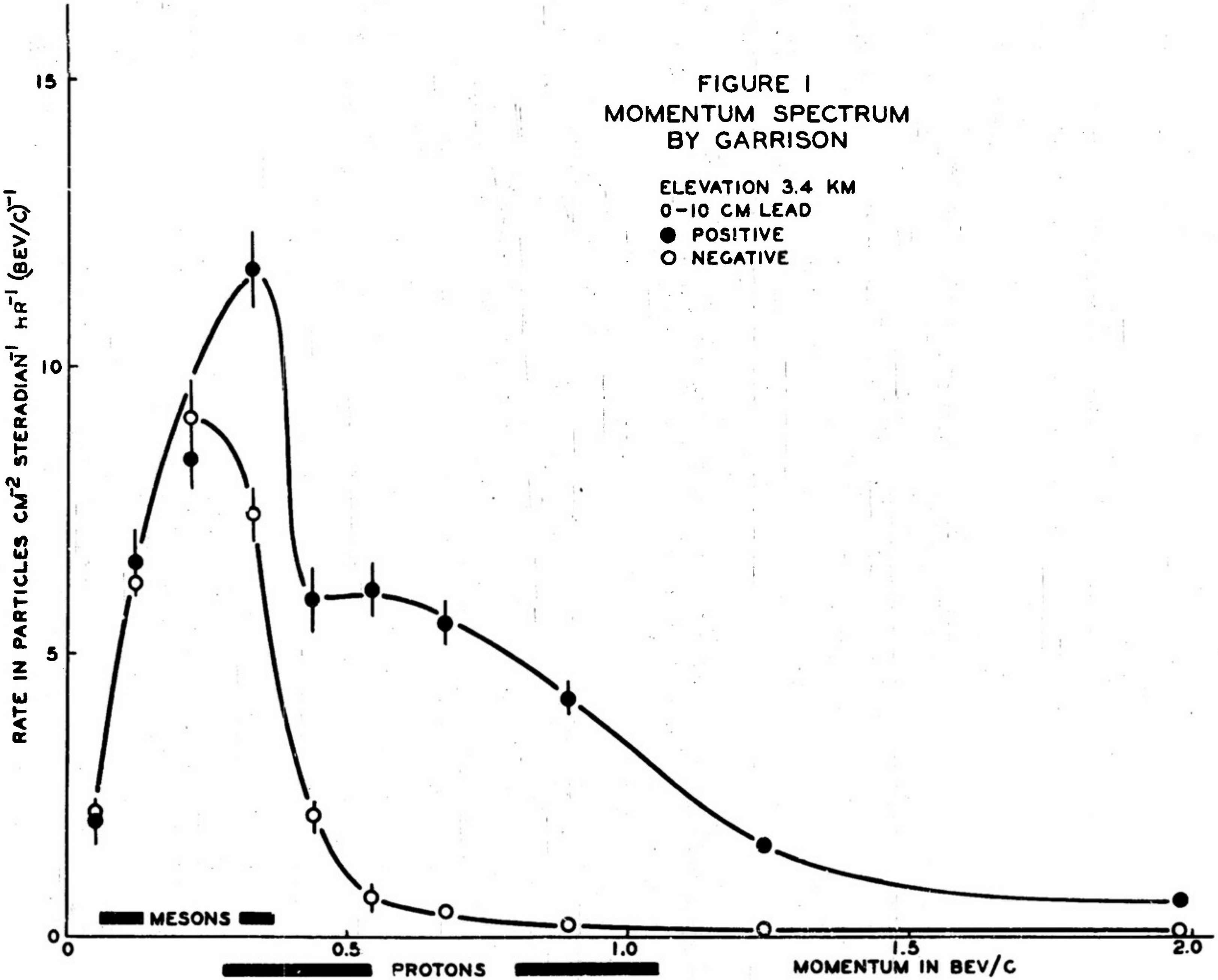

FIGURE I
MOMENTUM SPECTRUM
BY GARRISON

nuclear collisions.

The present experiment is concerned with the small but significant number of events in which negative particles were apparently stopped in the absorber even though they had momenta much greater than that corresponding to the ionization cut-off for mu mesons. While straggling, scattering, and the method of plotting data can account for inclusion of some mesons above 0.5 bev/c, these factors cannot account for the presence of small numbers of negative particles above 1 bev/c. This tail of negative particles was also observed in the momentum spectra obtained by Todd (9) at 3.4 km and sea level, and by Sandstrom (12) at 3.3 km.

It was not known to what source these events should be attributed. There was no assurance that they represented actual absorption rather than an instrumental error. Indeed, it was to be expected that due to counter dead time a small fraction of the total high momentum flux would be erroneously recorded as stopping in the absorber. As will be explained later, each discharge of a Geiger tube is followed by a brief dead time during which the tube cannot be discharged again. If a particle should pass through the Geiger tubes below the absorber during this dead time the tubes would not be discharged and the particle would be erroneously recorded as stopping in the absorber. While this could account for most of the apparent absorption of fast negative particles at sea level, the possibility still existed that at least some of these events represented true absorption. Such events could represent a small flux of negative protons, negative pi mesons, or other types of heavy mesons showing strong nuclear interaction, or could indicate a larger nuclear interaction cross section for mu mesons than was to be expected on the basis of other work.

Very little information is available concerning these various possibilities. No reliable evidence has been obtained for the existence of negative protons; the flux density of such particles at mountain altitudes and sea level is certainly small if present at all. Practically no information is available concerning the flux density of fast pi mesons. The usual identification techniques based upon momentum, ionization range and density, and scattering are not sensitive enough to differentiate between pi and mu mesons at the high momenta considered by these experiments. Attempts to identify fast pi mesons by means of nuclear collisions produced by them in nuclear emulsions are tedious and unreliable, and fail completely above about 1 bev due to the inability to differentiate between pi mesons and protons. It is known that because of the short decay time of the pi mesons the flux density must be small. Previous investigations of the nuclear interaction of mu mesons indicate that the interaction cross section of these particles is too small to account for the observed absorption of negative particles. The results of these investigations are ambiguous, however, due to the inability to make certain that the interacting particles are mu mesons. (See Chapter IV, Section D.)

Because of the lack of information concerning these particles and events, it seemed worth while to make a closer examination of the unexplained absorption of fast negative particles. By reducing the instrumental errors to a negligible amount, upper limits could be placed on the intensity of the particles and events listed above.

The experimental arrangement used in the present investigation is similar to that used in the previous investigations by this laboratory. The principal difference is that the leakage of particles through the anti-coincidence Geiger tubes below the absorber has been eliminated by suitable electronic circuits. These circuits prevent the recording of any events during the dead time following the discharge of any anti-coincidence tube. Furthermore, care has been taken that the tray of Geiger tubes below the absorber completely covers the beam of particles defined by the coincidence tubes C_1 and C_2, and that all Geiger tubes function efficiently throughout the experiment.

With the improved technique no events indicating that high energy negative particles stopped in the absorber were recorded at sea level. As will be shown later, the statistics and nature of the experiment were such that if as few as 0.02% of the negative particles had been stopped in the absorber they would have been detected. This result shows that the previously observed anomalous absorption of negative particles at sea level can be completely accounted for by instrumental errors. From the result of this experiment, one concludes that negatively charged particles having nuclear interaction cross sections comparable to that of the proton cannot constitute more than 0.05% of the total flux of negative particles at sea level.

CHAPTER II

THE EXPERIMENT

As stated in the introduction, the purpose of the present experiment was to make a search at sea level for negative non-electronic cosmic ray particles that stopped at ranges appreciably less than the ionization range of mu mesons of the same momentum. The sign of the charge and the magnitude of the momentum of ionizing particles that stopped in 10 cm of lead were determined by means of a counter-controlled cloud chamber operated in a magnetic field. A significant feature of the experimental technique was that the leakage of particles through the anti-coincidence tray due to inefficiency (resulting from the dead time of the Geiger tubes) was eliminated by suitable electronic circuits to be described in detail below. The experiment was conducted in Seattle during the summer of 1952.

A. Experimental Arrangement

A sketch of the experimental arrangement is shown in Figure II. Events were recorded in which Geiger tubes C_1 and C_2 were discharged in coincidence while all the anti-coincidence tubes of groups A_1 and A_2 failed to discharge. These events are called C-A events.

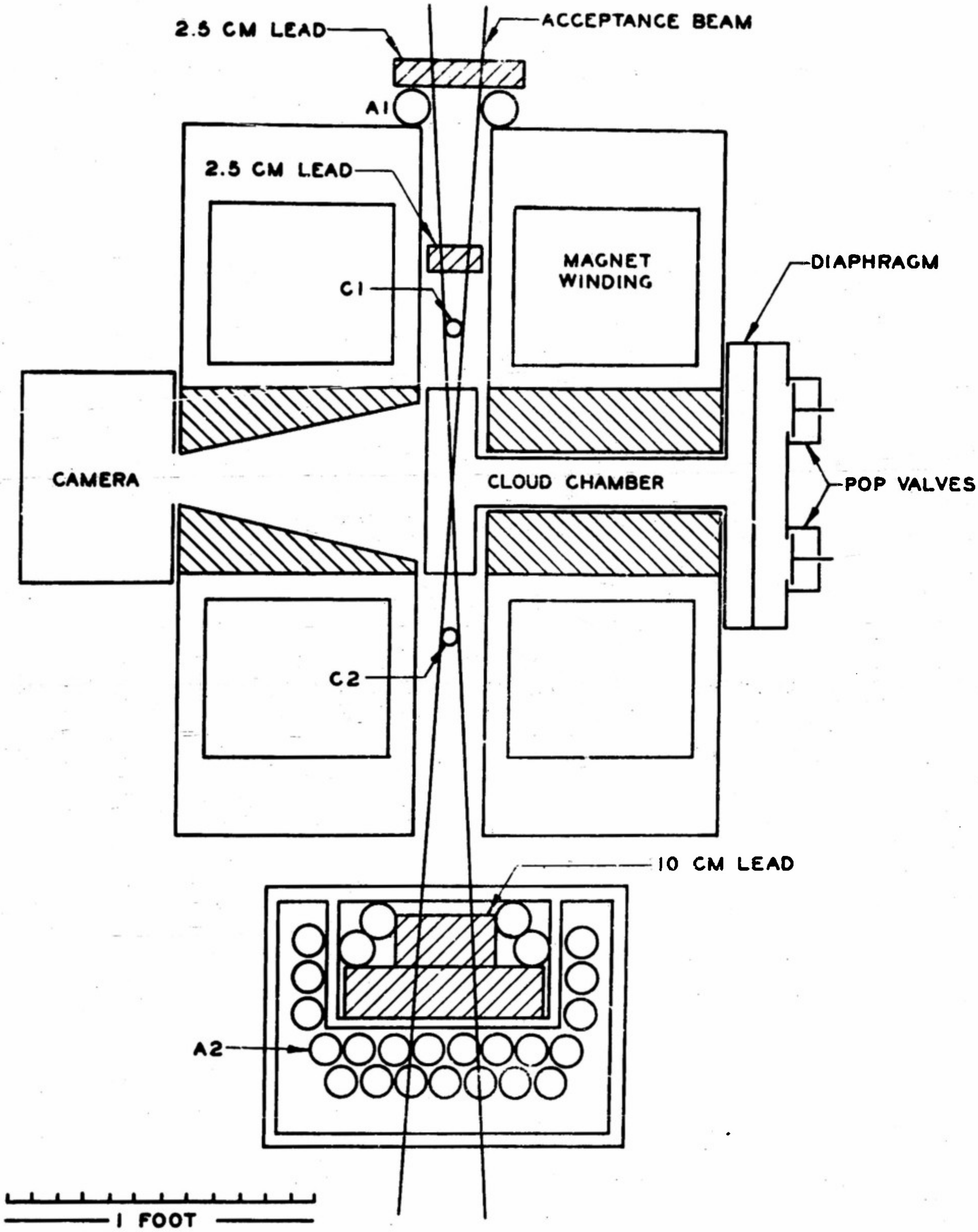

FIGURE 11
EXPERIMENTAL ARRANGEMENT

The Geiger tubes A_1 reduce the number of electron showers photographed, since these tubes are triggered by secondary cascade particles produced in the 2.5 cm lead block immediately above them. The most reliable method of detecting electron showers is the photographing of multiple tracks in the cloud chamber; therefore it is not essential that the anti-coincidence tubes give efficient shower protection. It is advantageous, however, to photograph as few showers as possible so that time is not wasted on irrelevant events. In previous experiments small anti-coincidence tubes were used between the magnet faces in close proximity with tube C_1. These small tubes proved unreliable, however, so in this experiment large tubes are used in a somewhat less advantageous position.

The 2.5 cm lead block above the tube C_1 provides more material close to the chamber and therefore increases the probability that energetic electrons will form showers showing multiple tracks in the chamber.

Those tubes of group A_2 which are located below the lead absorber form the principal anti-coincidence tray. These are the tubes that are fired by the ionizing particles that traverse the entire absorber. The tubes at the sides of the absorber give some protection against showers and prevent the recording of events in which high energy particles undergo wide angle scattering in the absorber. These tubes also decrease the probability of recording events in which high energy particles entering the absorber from the side undergo nuclear collisions in the lead absorber from which secondary particles pass upward through the cloud chamber and C counters.

B. The Equipment

The principal pieces of apparatus used in this experiment are essentially those used in previous experiments by this laboratory and are described in detail elsewhere (2). A brief description is given here of those components left unchanged; more detail is given on the components that have been altered.

The cloud chamber is 7 inches in diameter, 2.5 inches deep and has an illuminated depth of 1 inch. It is filled to a gauge pressure of 20 pounds/inch^2 with argon and the saturated vapor of a 60-40 n-propyl alcohol-water mixture. The chamber is operated in a magnetic field of 8,200 gauss produced by an electromagnet carrying a current of 800 amperes. The current is supplied by a motor-generator set delivering 26 kilowatts. The magnet sections are wound of solid copper conductors with a 0.25 X 0.80 inch rectangular cross section. The coils are cooled by forced oil flow, the oil in turn being cooled in an oil-water heat exchanger. The oil temperature is automatically controlled to within 0.01°C. The magnet current was adjusted manually and during the operating time of the experiment did not vary over 3%, which corresponds approximately to a 1% variation in the magnetic field.

In order to minimize the air gap between the magnet faces, the expansion mechanism of the chamber is mounted outside the magnet structure, the expansion taking place through a 1 1/4 inch brass tube 10 inches long which passes through the core of one of the magnet sections. The chamber is photographed through a conical hole through the core of the other magnet section.

The coincidence Geiger tubes C_1 and C_2 have glass envelopes containing a 6 inch section of 3/4 inch copper tube as a cathode and a 5 mil tungsten wire anode. To facilitate close packing, the anti-coincidence tubes are made with the copper cathode forming the outer wall. These tubes are 1 1/4 inches in diameter and 30 inches long. The effective length is somewhat less (about 28 inches) because of the seals and the glass shields which prevent the initiation of discharges at the sharp points of the connection between the anode wires and the lead wire.

The tubes were filled with argon and 10% (by volume) petroleum ether as a quenching agent. The filling pressure was adjusted so that the tubes started counting at about 1150 volts, which corresponds to about 13 cm of Hg for the anti-coincidence tubes. The tubes were operated near the center of the counting plateau at 1350 volts.

The 29 anti-coincidence Geiger tubes were fed into three anti-coincidence channels, each channel having its own preamplifier, but all channels being connected to the same C-A mixer. (The C-A mixer is the circuit that generates a voltage pulse whenever the coincidence tubes are discharged simultaneously while no anti-coincidence tube is discharged.) Since the success of the experiment depended critically on the efficient operation of the Geiger tubes, it was expedient to check their counting rates at frequent intervals. Arrangement was made to do this without interrupting the course of the experiment. It was found that not more than four anti-coincidence tubes should be scaled simultaneously, since the resultant high counting rate might mask an abnormal counting rate of an individual tube. A battery of switches was so arranged that the tubes could be scaled in groups of three while the output of the tubes being scaled continued to feed into an anti-coincidence channel. Twice each day during the experiment the tubes were scaled in groups of three for one minute.

The coincidence tubes C_1 and C_2 were also scaled twice each day. As an additional check on the continued efficient operation of the coincidence tubes, a continuous record was kept of the coincidence rate.

During the course of the experiment, only one coincidence tube and one anti-coincidence tube had to be replaced. However, due to a failure of one of the scaling switches, one roll of film (corresponding to seven days of operating time) had to be discarded.

C. Counter Dead Time

In previous experiments the inefficiency of the anti-coincidence tray was due in part to the dead time of the Geiger tubes. Due to the nature of the Geiger discharge, there is a brief period following each count in which a second ionizing particle traversing the tube will not produce a discharge because of the presence of a positive ion sheath surrounding the center wire. Following this completely inactive period while the positive ion sheath is moving toward the cathode, discharges can occur but will be of smaller magnitude than those occurring after complete recovery. As the anti-coincidence circuit requires some minimum voltage input, the effective dead time will be determined both by the structure of the Geiger tube and the constants of this circuit.

The effective dead time of the tubes used in this experiment was measured by observing the Geiger pulses on a Tektronix oscilloscope while a radium sample gave a high counting rate. The horizontal linear sweep of the oscilloscope was set to be triggered only by Geiger pulses of maximum size, the voltage across the tube appearing as the vertical deflection. The lapse of time between the peak of a pulse of maximum size and the occurrence of a pulse of sufficient size to actuate the electronic circuit was found to be about 450 microseconds. The dependence of the recovery time on the operating voltage is indicated by the following data.

Voltage	Effective Dead Time
1320 volts	500 μsec
1355	450
1380	400

The Geiger tubes were maintained at 1355 volts within 1%. It is evident that a blanking pulse which prevents the recording of a C-A event for a period of 600 microseconds after the discharge of any anti-coincidence tube will prevent the recording of spurious events due to leakage resulting from counter dead time.

The circuits for generating and applying the 600 microsecond blanking pulse are shown in Figure III. The C-A mixer circuit, using tubes T24 and T25, is a standard Rossi type circuit. Since the resistances of tubes T24 and T25 in the conducting state are smaller than the 25K plate resistor, the plate voltage of these tubes remains nearly constant as long as one or both of the tubes are conducting. However, when both tubes are cut off, the plate voltage rises sharply to the supply voltage, thus generating the C-A pulse. In the normal configuration, tube T25 is conducting while T24 is non-conducting. If a negative coincidence pulse (C pulse) cuts off tube T25 at a time when T24 is still nonconducting a C-A

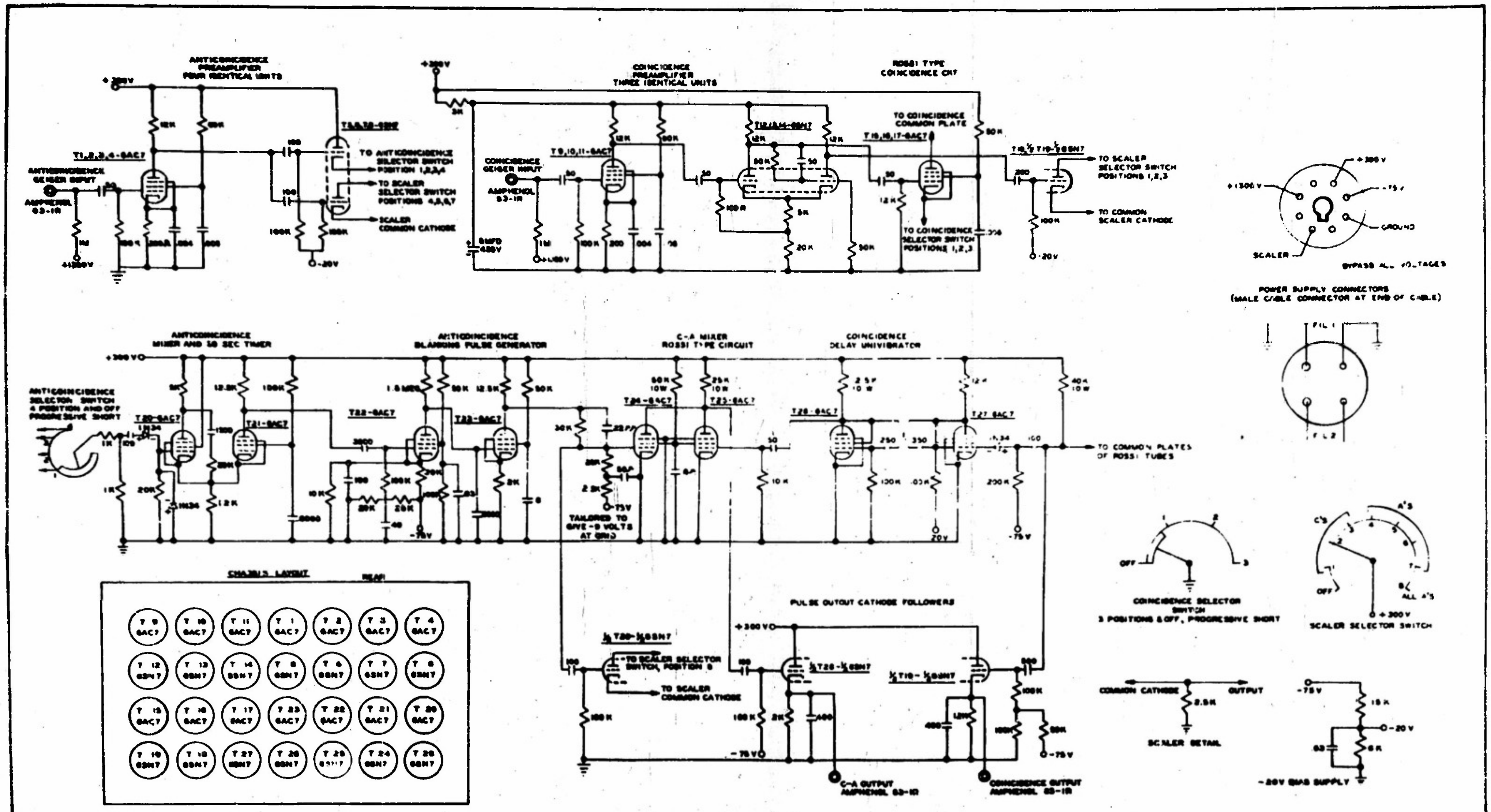

EVENT SELECTOR

FIGURE III

pulse is generated; however, if tube T24 is conducting when the C pulse cuts off tube T25 no pulse is formed. In order to prevent the production of C-A pulses during the recovery time of the Geiger tubes, it is necessary, therefore, to apply a positive blanking pulse to the grid of tube T24 which causes it to conduct for about 600 microseconds after the discharge of any anti-coincidence Geiger tube.

The blanking pulse is generated by discharging the 6,000 mmfd condenser through tube T22, the duration of the pulse depending upon the rate of recharging the condenser through the 1.2 megohm plate resistor. It was found that the anti-coincident pulses applied to the control grid of tube T22 were so short that the tube did not remain conducting long enough to permit the condenser to discharge sufficiently to produce a blanking pulse of 600 microseconds. Therefore the anti-coincidence pulses (A pulses) were lengthened to 30 microseconds by means of the univibrator using tubes T20 and T21. The negative 600 microsecond pulses are inverted and amplified by tube T23 before being applied to the control grid of T24 of the mixer circuit. To ensure that the blanking pulse is in effect (that is, that tube T24 is conducting) when the coincidence pulse arrives at tube T25, the C pulse is delayed 35 microseconds by the circuit employing tubes T26 and T27.

An important feature of the blanking pulse circuit is that every anti-coincidence pulse arriving from the 30 microsecond timer triggers a full 600 microsecond blanking pulse no matter how closely the A pulses follow one another. This is not true, however, for the 30 microsecond univibrator. If an A pulse arrives at tube T20 within 30 microseconds of the preceding A pulse, the univibrator is not retriggered. For this reason the effective blanking pulses range from 570 to 600 microseconds. However, because of the wide margin between the length of the blanking pulse and the observed Geiger tube recovery time (450 microseconds) this range of values is of no significance.

As will be discussed later, the effect of introducing this blanking pulse is only to reduce by about 4% the total effective time of observation. During the effective time of observation it in no way reduces the probability of detecting those particles stopping in the absorber.

D. Track Selection

This experiment is primarily concerned with singly occurring non-electronic particles that stop in 10 cm of lead. These are recorded as C-A events by the electronic circuits, and (except during the "inactive time" discussed below) trigger the cloud chamber expansion. However, since all C-A events are not caused by the absorption of singly occurring particles, it is necessary to stipulate further criteria which must be satisfied by a cloud chamber photograph to be included in the pertinent data.

To make virtually certain that no electron track would be included in the data, all those photographs showing more than one time coincident track were recorded as showers and were not considered in the determination of intensities or momentum spectra. This criterion leads occasionally to errors of exclusion because of the appearance of knock-on electrons and because of the accidental coincidence of non-related particles. The number of such errors is small compared with the total number of recorded events, as is shown in Chapter III.

Only those tracks were retained in the data which were produced by particles contained within the acceptance beam defined by the coincidence counters. As an aid in determining whether or not a particular trajectory was within the acceptance beam, a template representing the spacing and effective length of the coincidence tubes was mounted on the comparator described in the next section, the scale of the template being carefully matched to the magnification of the optical system. The effective length of the coincidence tubes is discussed in detail below. Since the entire acceptance beam is contained within the illuminated region of the cloud chamber, those tracks that passed out of the illuminated region, either toward the front or the back of the chamber, were discarded.

Finally only those tracks were retained whose width indicated that the passage of the particle was time coincident with the chamber expansion.

All those tracks fulfilling the requirements above are called "single tracks." Of the single tracks, those occurring near the chamber wall are not suitable for curvature measurement because of the track distortion due to turbulence in the gas near the wall and because of the shortness of the track. The single tracks are therefore divided into two groups; the "measured tracks" being all those whose lengths are more than 75% of the chamber diameter, the "short tracks" being those that do not satisfy this length requirement. The sign of the charge and the magnitude of the momentum of each particle producing a "measured track" were recorded.

It is important to note that with the exception of the requirement that only a single track appear in the cloud chamber, the track selection criteria in no way bias the observation of particles of a specific type.

E. Momentum Measurement

The momenta of those particles triggering the cloud chamber and satisfying the track selection rules discussed in the preceding section were found by determining the radius of curvature of the particle's path through the cloud chamber.

The expression $P = 300$ HR gives the momentum P (in ev/c) in terms of the magnetic field H (in gauss) and the radius of curvature R (in centimeters). As described elsewhere (2), the radius of curvature of each trajectory was determined by comparing the photograph of the cloud chamber track with a set of standard curves. A machinist's comparator was specially adapted for this task. The set of standard curves was made by first scribing a set of 19 curves of known radii ranging from 0.3 to 10 meters on a glass plate coated with Aqua-Dag. This plate was then photographed by the same camera used in photographing the cloud chamber. An enlargement of this photograph was made by projecting it in the comparator and replacing the ground glass viewing screen by a photographic plate. A contact print made from this plate served as the set of standard curves. The curvature measurement was performed by projecting the cloud chamber photographs on the viewing screen of the comparator and finding the standard curve which most nearly fit the track curvature. For convenience in recording, the standard curves were labeled by letters from A to X.

Since the set of standard curves and the cloud chamber photographs passed through identical optical treatment, any error in the optical system would affect both in the same manner and therefore not alter the curvature measurement--<u>provided</u> that the plate carrying the set of standard curves is used in the same orientation in which it was originally printed. The work of Charbonnier (3) has shown that an error equivalent to a radius of curvature of 40 meters was present in the optical system and was of such a nature that curves convex upward on the screen are increased in curvature. Since the standard curves were originally printed convex upward, their curvature has been increased by the error. Photographs of cloud chamber tracks convex downward on the viewing screen are decreased in curvature; consequently the error introduced by comparing these tracks with the standard curves is twice as large as the error in the optical system. Therefore, while no correction is necessary for tracks convex upward, the observed curvature of those tracks convex downward must be corrected by increasing the curvature by an amount corresponding to a radius of curvature of 20 meters. This correction has been applied to the data given below.

F. Counter Telescope Admittance

A meaningful presentation of the experimental results requires that they be expressed in terms of an absolute intensity I so defined that the expression I da dw dt gives the number of particles incident on an area da within the solid angle dw oriented perpendicular to da within a time interval dt. For isotropic radiation the admittance A of a counter telescope is defined as the integral of da dw over the effective dimensions of the tubes making up the telescope. At sea level the cosmic radiation varies approximately as the square of the cosine of the zenith angle; the effective admittance of a counter telescope oriented vertically is therefore given by the integral of $\cos^2\theta \, da \, dw$ taken over the effective area of the tubes. Carrying out this integration and discarding terms of higher order than $(D/H)^2$ and $(L/H)^2$ the effective admittance is given approximately by:

$$A = \frac{D^2L^2}{H^2}\left(1 - \frac{D^2}{2H^2}\right)\left(1 - \frac{L^2}{2H^2}\right)$$

where L and D are the effective length and diameter and H is the distance between corresponding planes of the tubes.

The counters forming the telescope are 12 inches apart, 6 inches long and 3/4 inches in diameter. Street and Woodward (5) have shown that the tube diameter can be taken as the effective width of the Geiger counter with negligible error. Due to the fringing of the electric field at the ends of the cathode, however, the effective length of the tubes is somewhat greater than the geometrical length. The effective length was found experimentally by plotting the number of cloud chamber tracks as a function of the angle between the vertical and the path of the particle. Since Charbonnier (3) investigated those particles penetrating 239 g/cm^2 of lead, the tracks photographed in that experiment were very nearly straight and therefore well suited for angular measurements. Furthermore, since the geometrical arrangement, the filling of the Geiger tubes, and the Geiger voltage were the same in both experiments, the effective length determined from Charbonnier's data is valid for the present experiment.

Figure IV shows the plot of the angular distribution, the indicated errors being standard deviations. The maximum angle between the vertical and the paths of the particles passing through the telescope is taken as the intersection of the smooth curve with the horizontal axis, and is seen to be about 30°. The corresponding effective length for the Geiger tube is 7.0 inches. Using this value for the effective length and the geometrical diameter for the effective width of the Geiger tubes, the admittance of the counter telescope is found to be 1.00 cm^2 steradian.

Since the photographed region of the cloud chamber has a diameter of only 5.35 inches, the entire beam defined by the telescope is not available for study. The effective admittance must be corrected by an amount corresponding to the beam defined by that portion of the C tubes extending beyond the photographed region of the cloud chamber. With this correction, the effective telescope admittance is 0.97 cm^2 steradians.

This value of the admittance may be compared with that found previously by Charbonnier. By comparing the intensity of the hard component as detected by this equipment with the absolute intensity of the hard component as determined by Rossi, Charbonnier found an admittance of 0.94 cm^2 steradians, in good agreement with the value found here.

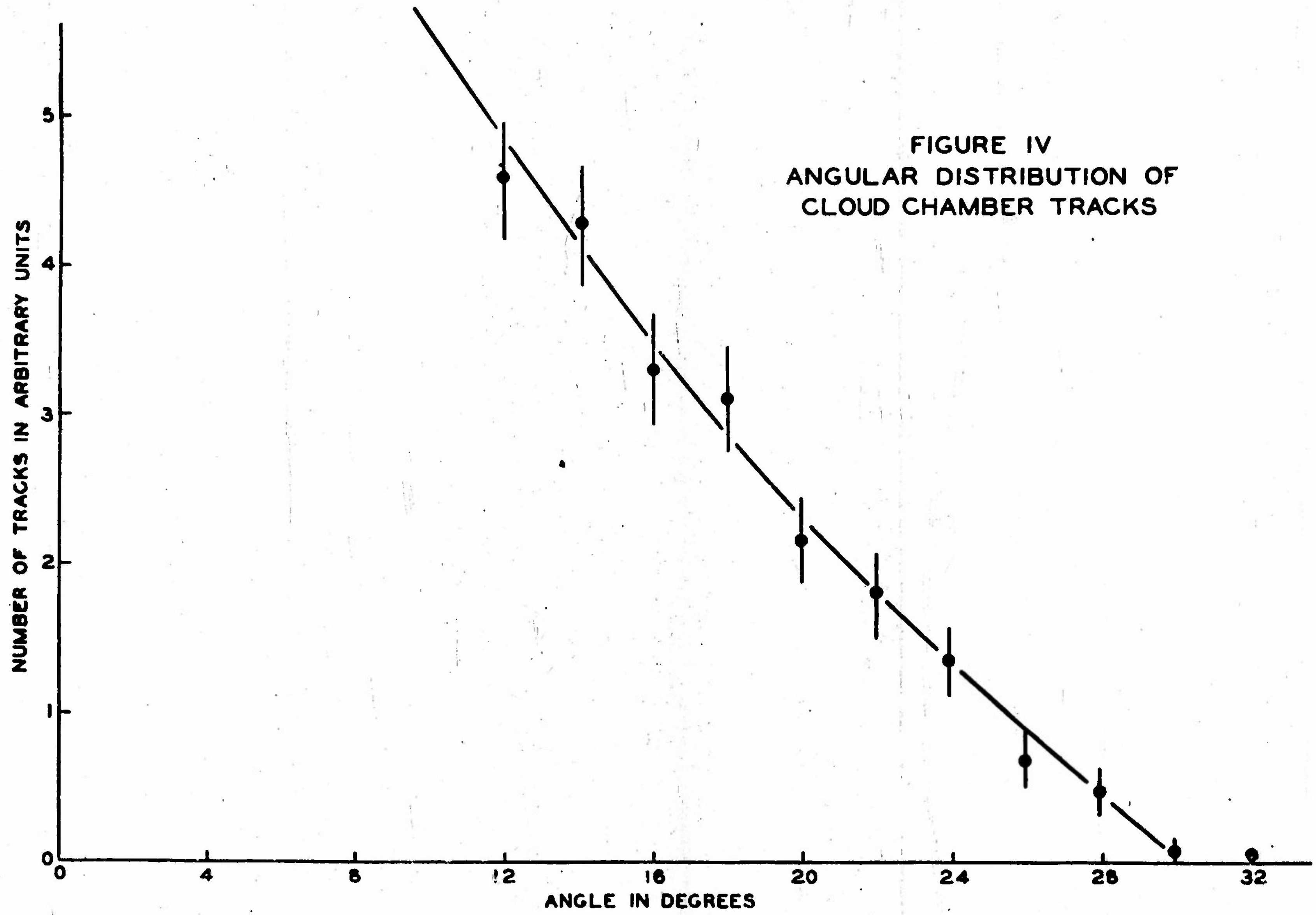
FIGURE IV
ANGULAR DISTRIBUTION OF
CLOUD CHAMBER TRACKS
NUMBER OF TRACKS IN ARBITRARY UNITS
0
1
2
3
4
5
0
4
8
12
16
20
24
28
32
ANGLE IN DEGREES

G. Normalization

The conversion of the experimental data to absolute intensities requires not only a knowledge of the admittance A , but also a knowledge of the rate at which singly occurring particles passed through the counter telescope and stopped in the absorber below the chamber. This "single track rate" can be determined from the rate of occurrence of C-A events by making the natural assumption that the distribution of event types (showers, misses, single tracks) is the same whether or not the cloud chamber is "active." The cloud chamber is active during the time in which the control circuits are in such a configuration that a C-A event would trigger an expansion. It is not active during the 90 second sterilization period which permits the chamber to return to equilibrium after each expansion, and during the time required for inspection and adjustment of the chamber. Although the number of C-A events occurring during the inactive time were registered, further information concerning these events was not available, since cloud chamber photographs were not taken.

The C-A rate was determined from the total registered number of C-A events and the time during which the equipment was operated. Since no C-A events could be recorded during the 600 microsecond pulse following the discharge of any anti-coincidence tube, the time of operation was corrected by multiplying the total time by the fraction of time during which the blanking pulses were not in effect. The rate of generation of the blanking pulses (found by scaling the output of tube T23 in Figure III) was $59.5 \pm .4$ pulses per second; since the blanking pulses were 600 microseconds long, they were in effect, on an average, 0.036 seconds during each second of operation. The corrected time is found by multiplying the total time by $\frac{1 - 0.036}{1} = 0.964$, i.e., by the fraction of time during which the blanking pulses were not in effect.

The single track rate T is given by the expression $T = RS/P$, where R is the C-A rate, S is the number of photographs showing single tracks, and P is the total number of photographs.

The absolute directional differential intensity is defined by the expression $J(p) = N(p)/da\ dt\ dp\ dw$, where $N(p)$ is the number of particles in the momentum interval dp with mean momentum p that pass through an area da within a solid angle dw normal to da within a time dt. In terms of the experimental data, $J(p)$ is given by $J(p) = TL(p)/AM \Delta p$, where T is the single track rate, A is the telescope admittance, and $L(p)/M$ is the ratio of the number of measured tracks in the momentum interval ΔP with mean momentum P to the total number of measured tracks.

CHAPTER III

DATA AND RESULTS

A. Experimental Data

The experimental data are listed in Table I. The term "time" refers to the time during which the Geiger counter system was operating and has been corrected for the 600 micro-second blanking pulse, as discussed in Chapter II. The term "straight tracks" refers to those tracks whose radii of curvature were too great to be measured. "Misses" refer to those photographs (or "frames") which show no tracks at all. The heading "Letter Group" refers to the standard curves discussed in Chapter II, Section E. The first letter group (-A) includes all particles with momenta less than the momentum corresponding to standard curve A. The other terms have been defined in the sections on track selection and normalization.

With one exception, all tracks whose radii of curvature were determined have been grouped in the indicated momentum intervals. The one track that has not been included is discussed in detail in Section B. The momenta and momentum intervals for the negative particles have been corrected for the 40 meter error in the radius of curvature measurement discussed in Chapter II, Section E. The intensities for the

TABLE I: EXPERIMENTAL DATA

Range of Particles	: 0-10 cm of lead
Elevation	: sea level
Geomagnetic Latitude	: 53° N
Location	: Seattle

Positives	795	Showers	1864
Negatives	553	Misses	2269
Straight Tracks	11	Total Frames	5647
Total Measured	1359	Time in Hours	1399
Short	155	C-A Events	7258
Total Single Tracks	1514		

Letter Group	Number of Particles	Average Momentum in bev/c	Absolute Intensity in particles per cm^2 sterad hr bev/c	
		Positive Particles		
-A	32	0.04	0.46	± 0.07
A-C	71	0.10	1.65	0.19
C-F	120	0.16	2.34	0.21
F-I	214	0.23	2.90	0.20
I-K	115	0.31	1.77	0.16
K-M	49	0.39	0.65	0.09
M-P	41	0.52	0.28	0.04
P-S	55	0.74	0.23	0.03
S-U	55	1.04	0.19	0.03
U-W	27	1.53	0.05	0.01
W-X	10	2.18	0.02	0.01
		Negative Particles		
-A	72	0.04	1.05	± 0.12
A-C	90	0.10	2.22	0.23
C-F	121	0.15	2.53	0.23
F-I	208	0.22	3.10	0.21
I-K	52	0.29	0.89	0.12
K-M	10	0.36	0.15	0.05
M-P	0	0.48	0.00	
P-S	0	0.67	0.00	
S-V	0	0.86	0.00	
V-W	0	1.06	0.00	
W-X	0	1.62	0.00	

various momentum intervals have been computed as described in Chapter II, Section G.

The differential momentum spectra, plotted separately for negative and positive particles, appear in Figure V. The most striking feature of the data is that, with the single exception discussed in Section B, no negative particle with momentum greater than 0.37 bev/c was recorded. This result and the conclusions that can be derived from it are discussed quantitatively below.

As in Figure I, the heavy bars marked "mesons" and "protons" at the bottom of the graph show for each of these particles the momentum interval corresponding to the ionization-range interval determined by the equipment. The minimum ionization range is determined by the amount of material separating the sensitive volumes of the cloud chamber and lower coincidence tube of the counter telescope. This material, about 2.5 g/cm^2 lead equivalent, corresponds to a minimum meson momentum of 0.05 bev/c and a minimum proton momentum of 0.25 bev/c. The upper momentum limit for particles stopped by ionization in the absorber below the chamber is determined by the amount of material separating the sensitive volumes of the cloud chamber and the Geiger tubes forming the anti-coincidence tray below the absorber. For a particle passing vertically through the equipment, this material amounts to 10 cm of lead plus enough glass, copper and

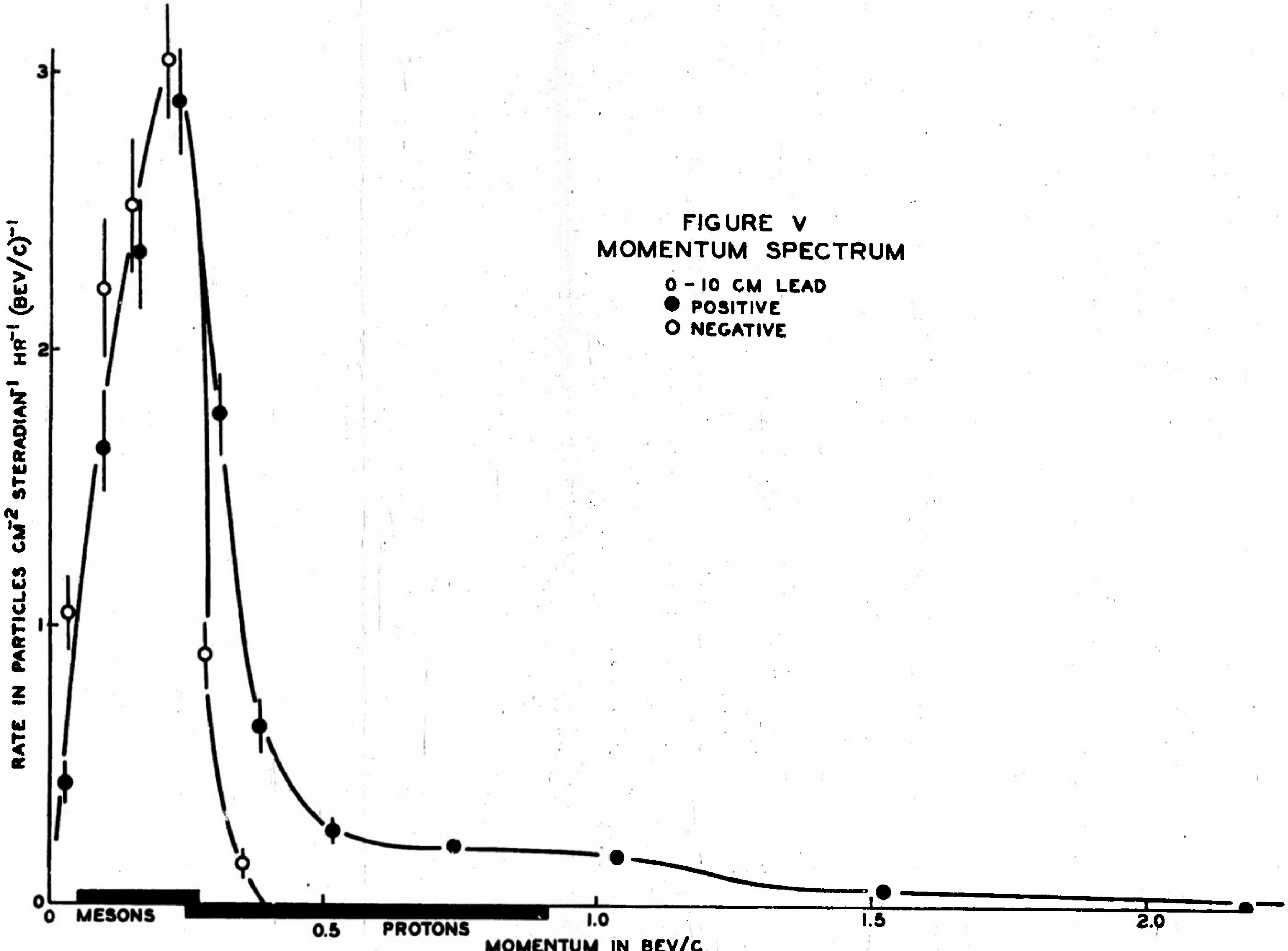

FIGURE V
MOMENTUM SPECTRUM

steel to make a total of 147 g/cm^2 lead equivalent, which corresponds to momenta of 0.27 bev/c for mesons and 0.90 bev/c for protons. Due to the spread in zenith angle of the particle trajectories and to multiple scattering within the absorber, there is a distribution of path lengths in the material and the upper momentum cutoff is consequently poorly defined. The observed maximum momentum for mesons is about 0.1 bev/c greater than the indicated value.

Since fast positive and negative mesons have the same momentum-range relationship, the momentum spectrum for positive particles above 0.37 bev/c cannot be attributed to mesons. Previous investigations have shown that the positive particles with momenta above the meson cutoff obey the momentum-range relationship for protons, and are therefore assumed to be protons. The proton spectrum does not go to zero beyond the upper ionization cutoff because some energetic protons are stopped in the absorber by catastrophic nuclear collisions (1,9).

B. An Exceptional Track

The only cloud chamber track observed in the experiment which satisfied all the requirements of a "measured track" but was nevertheless excluded from the data is shown in Plate I (a). The momentum of the particle (if singly charged) was 0.54 bev/c, and the direction of curvature is such that if the

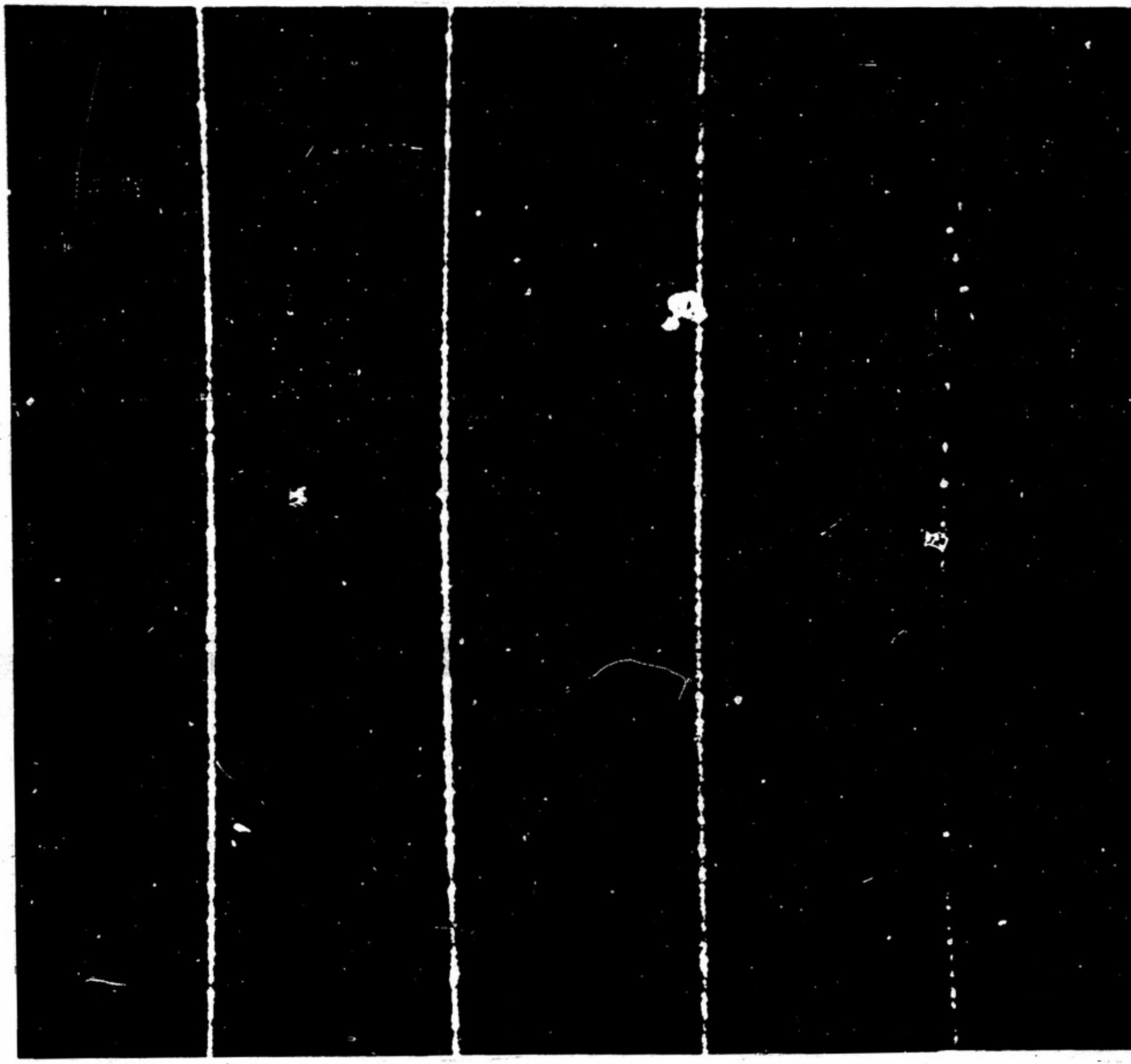

a b c d

PLATE I.

particle traveled downward through the chamber, it must have been negatively charged. This particle was excluded from the data because its heavy ionization indicates that the particle has a mass greater than any known negatively charged particle, and therefore presumably was a positive particle passing upward through the chamber.

A precise value of the ionization density of the track cannot be given, but an estimate may be made by comparing the track with tracks produced by protons of known momenta. (Unfortunately, much detail has been lost in the photographic reproduction of the tracks in Plate I. The arguments given here are based on the appearance of the tracks on the screen of the comparator.) Track (c) of Plate I was produced by a 0.54 bev/c proton. Since the unusual track (a) is definitely denser than the proton track (c), and since both tracks were produced by particles with the same momentum, the particle that produced track (a) must have been heavier than a proton.

Track (b) was produced by a 0.37 bev/c proton, which has a specific ionization of 6.5 times minimum. (Track (d) is a minimum ionization track.) Comparison of tracks (a) and (b) indicates that track (a) has a density of at least 6.5 times minimum and perhaps more. This means that the particle that produced track (a) was at least 1.5 times as heavy as a proton.

All of the tracks shown in Plate I were obtained within an interval of about 15 hours. Although cloud chamber conditions might have been slightly different for the various tracks, the marked variations in track densities could not be accounted for in this way.

The following table lists the most likely particles that might have produced the unusual track. Also shown are the momentum in bev/c as indicated by track curvature, the ionization density in terms of minimum ionization, and the range of the particles in g/cm^2 of lead equivalent. The last two quantities are predicted by collision theory from the measured momentum.

Particle	Proton	Deuteron	Triton	Alpha Particle
Momentum	0.54	0.54	0.54	1.08
Ionization	3	11	25	47
Range	32	3.5	0.9	0.9

As mentioned in Section A, the minimum range required for a particle to leave the sensitive region of the cloud chamber and to trigger the second tube of the counter telescope is about 2.5 g/cm^2. (This minimum range is required for particles moving upward through the chamber as well as for those moving downward.) The unusual track could not have been produced by a particle heavier than a deuteron, since these particles do not have the required minimum range. As mentioned above, the possibility that the particle was a proton can be eliminated on the basis of track density.

The only definite conclusion that can be drawn concerning the identity of the particle is that it is heavier than a proton but lighter than a triton. The particle conceivably could have been a negative particle with mass greater than a proton, but there is no convincing evidence for the existence of a particle of this type, with the possible exception of the negative V particle. It is doubtful that the V particle has a mass great enough to produce a track like the one shown in Plate I (a), and the extremely short decay time of this particle makes it unlikely that it would be detected with this equipment (6,7,8). A more credible explanation of the track is that it was produced by a deuteron moving upward through the chamber. It is rather unexpected that a deuteron of this momentum (corresponding to a kinetic energy of 80 mev) should be moving upward. Particles evaporated isotropically from an excited nucleus usually have energies much less than 80 mev, while high energy particles emitted in a nucleon-nucleon collision are usually emitted in the forward direction (and therefore downward for cosmic rays at sea level). There is, of course, no sharp division between the two processes; nucleon-nucleon collisions have the effect of adding a high energy tail on the distribution of particles emitted by evaporation. Camerini et al (14) and others have studied the low energy singly charged particles (protons, deuterons and tritons) emitted in stars produced in nuclear emulsions. It was found that practically all these particles have energies less than 30 mev for protons (60 mev for deuterons) and that they are distributed isotropically. Roughly a third of the particles were found to be deuterons and tritons. These findings are in fair agreement with the theory of nuclear evaporation as extended by Le Couteur (28). According to this theory, for an excitation energy of 650 mev the probability of emitting an 80 mev deuteron is less than that of emitting a deuteron of the most probable energy (about 7 mev) by a factor of the order of 10^{-5}.

A more probable origin of an 80 mev deuteron is suggested by the investigations by Camerini et al of the "grey tracks" associated with stars in nuclear emulsions. These tracks are produced by singly charged particles with energies from 25 to 500 mev (for protons). These particles presumably escape from the nucleus before the excitation energy has become statistically distributed among the nucleons. It was found that about 22% of these particles are deuterons and tritons. Most of the grey tracks are in the forward direction with respect to the incident particle, the degree of collimation increasing with increasing energy. For proton energies of 60-80 mev the mean angle of emission is 70° and the distribution is such that about 1/4 of the particles are emitted with angles greater than 90°. The authors point out that this angular distribution indicates that most of the particles are not knocked-on directly by the primary particle but rather by intermediary nucleons. It seems probable that the 80 mev deuteron observed in this experiment originated in such an event. According to the work of Camerini et al, the probability of observing a fast upward moving deuteron is only 1/5 that of observing a proton. Since only one fast particle was observed to move upward in the present experiment, little significance can be placed on the observation that it was a deuteron rather than a proton.

C. Statement of Results

In this experiment no negative particles (with the possible exception discussed above) in the momentum interval 0.37-1.65 bev/c were found to stop in 10 cm of lead. If the absolute intensity were such that one would expect on the average to have detected one such particle during the course of the experiment, the probability of the actual result (i.e., of detecting no such particles) would be 37%. An upper limit for the absolute intensity of such particles at sea level is computed on the basis that on the average one particle would be detected during the course of the experiment. In this way, using the normalization procedure discussed earlier, an upper limit of 1.0×10^{-3} particles/cm^2 sterad hr is found. That is to say, the absolute intensity of negative particles in the momentum interval 0.37-1.65 bev/c that are absorbed in 147

g/cm^2 of lead equivalent is $(0.0\ ^{+1.0}_{-0.0}) \times 10^{-3}$ particles/cm^2 steradian hr.

D. Validity of Results

Before confidence can be placed in the results stated above, it must be demonstrated that energetic negative particles would have been detected if they had passed through the counter telescope and been absorbed in the lead. That this equipment detects, within a few percent, all particles passing through the telescope is shown by the agreement between the value of the admittance found from the geometry of the telescope and the value deduced by Charbonnier. As discussed in Chapter II, Section F, Charbonnier's value was based upon a comparison of the intensity of the hard component as detected by this equipment with the absolute intensity given by Rossi. As a by-product of this experiment, the absolute momentum spectra of mu mesons with ionization ranges 2.5-147 g/cm^2 of lead and of protons with momenta less than 2.5 bev/c were obtained (Figure V). These spectra agree with those obtained by Todd (9) at sea level and show that the apparatus was functioning properly during the course of the experiment. There is nothing in the nature of the apparatus or track selection criteria that would discriminate against negative particles in the momentum interval considered in this experiment.

The momentum interval (0.37-1.65 bev/c) considered by this experiment is determined by the following considerations. The lower limit of the interval is fixed by the greatest momentum observed for negative particles that stopped in the absorber. As mentioned earlier, this momentum is about 0.1 bev/c greater than the momentum corresponding to an ionization range of 147 g/cm^2 of lead. The upper limit of the interval is the greatest momentum that can be measured by this equipment with negligible probability of mistaking the direction of curvature. The determining factor in the selection of the minimum path length for measured tracks was that tracks with radii of curvature less than 6.7 meters (corresponding to momenta less than 1.67 bev/c) should be clearly distinguishable from "straight tracks," i.e., tracks with no appreciable curvature. Tracks with radii of curvature greater than 6.7 meters were not considered in this experiment, and no attempt was made to determine the sign of the charge of the particles producing them.

CHAPTER IV

DISCUSSION OF RESULTS

A. Introduction

In a number of experiments performed by this laboratory (1,2,3,10,11,12) the composition of the cosmic radiation at lower altitudes has been studied. From these and many other studies it is clear that the radiation consists principally of an electronic component (electrons, positrons and photons), positive and negative mu mesons, protons and neutrons. While the vast majority of all particles constituting the radiation at lower altitudes are included in the above list, other types of particles are known to exist in small numbers. Thus in the determination of proton intensity made by this laboratory small numbers of deuterons and alpha particles were recognized through their ionization density. The radiation is known also to include pi mesons and a variety of other particles of very short life times such as V particles and τ and k mesons. In general these particles are found in association with high energy events (penetrating showers). No estimate is available for the absolute intensity of such particles. Because of their very short half lives such particles will be found only near their point of production and will contribute little to the general cosmic ray flux. The possibility also exists that the radiation contains small numbers of negatively charged protons.

The present experiment was intended to place limits on the total intensity of certain minor constituents of the total radiation. The technique would not detect particles of very short half life since they would have to travel at least a foot to actuate the counter telescope. In any case, as has been pointed out, such particles contribute very little to the total flux unless produced locally in very large numbers. The principal result of the present experiment is contained in the statement that the sea level radiation cannot contain a total intensity of negative particles exceeding 1.0×10^{-3} particles/cm^2 steradian hr, where reference is made only to those non-electronic negative particles in the momentum interval 0.37-1.67 bev/c and which are of such nature that they are absorbed in 147 g/cm^2 of lead. Stated differently, the total intensity of such particles in this momentum interval is less than 0.02% of the negative mu meson intensity in the same interval.

A variety of particles and events could contribute to the radiation whose total intensity is limited as above. In particular this would include pi mesons, negative protons, negative mu mesons absorbed through catastrophic nuclear interaction, and possibly other types of mesons. With respect to negative protons, if one assumes that they behave in the same manner as ordinary protons in so far as this experiment is concerned, it is found that their intensity cannot exceed 2.5×10^{-3} particles/cm^2 steradian hr for the momentum interval 0.69-1.75 bev/c. Conclusions regarding the intensity of pi mesons and the nuclear interaction of mu mesons will be discussed in more detail in the following sections.

B. Intensity of Pi Mesons

We define a removal path length in the following way. The expression $J_0 - J(x) = J_0[1 - e^{-x/L}]$ expresses the intensity $J_0 - J(x)$ of particles that are "removed" in an absorber distance X in terms of the intensity J_0 of particles incident on the top of the absorber and the removal path length L. An event is recorded as a "removal" only if all ionizing secondary particles as well as the primary particle are stopped in the absorber. The removal path length is therefore always equal to or longer than the mean path for nuclear interaction.

The nuclear interaction cross section of pi mesons has been investigated by means of counter systems, cloud chambers and nuclear emulsions. The results of these investigations have been summarized by Camerini et al (Chap. I, ref. 13) and show that within the statistical accuracy of the experiments the nuclear interaction cross section is the same as that for protons, approximately 80% of the geometrical nucleon cross section. Nuclear emulsion experiments by Camerini et al (14) also show that (at least up to about 1 bev) pi mesons as well as protons undergo nuclear collisions in which on the average a large fraction of the energy of the incident particle is distributed among several heavily ionizing particles. It therefore follows that pi mesons and protons should have approximately the same removal path length.

In a previous experiment, Garrison (1) has shown that protons with momenta less than 2.5 bev/c have a removal path length of 206 ± 30 g/cm^2. This value has been assumed for the removal path length of pi mesons. In Chapter III it was shown that the intensity of negative particles in the momentum interval considered by this experiment that stop in an absorber thickness of 147 g/cm^2 is less than 1.0×10^{-3} particles/cm^2 steradian hr. Using the expression given above in defining the removal path length, it is found that the intensity of negative pi mesons in the stated momentum interval that are incident on the absorber below the chamber cannot be as great as 1.9×10^{-3} particles/cm^2 steradian hr. Since these particles have passed through 60 g/cm^2 of material before entering the chamber, the intensity of pi mesons passing through the chamber is less than the intensity in the atmosphere above the equipment by a factor of $e^{-\frac{60}{206}}$. Including this effect and the decrease in momentum due to energy loss through ionization in the absorber above the chamber, the final result is that in the momentum interval 0.45-1.75 bev/c, the intensity of negatively charged pi mesons is less than 2.5×10^{-3} particles/cm^2 steradian hr.

In deriving this result the production of pi mesons in the absorber above the chamber has not been considered. Pi mesons produced in the absorber would probably be accompanied by secondary particles and so be overlooked because of the "single track" criterion used in data selection. In any case, such production could only add to the observed intensity and so does not affect the upper limit given.

In order to compare the results of this experiment with the results of others, it is convenient to express them in terms of the total intensity of mu mesons in the momentum interval considered. This total intensity can be found by integrating Rossi's (15) sea level momentum spectrum for mesons from 0.45 to 1.75 bev/c. It is found that the intensity of mesons in this momentum interval is 11.0 particles/cm^2 steradian hr. Puppi and Dallaporta (Chap. VI, ref. 13) have summarized the results of several determinations of the positive to negative ratio for mu mesons at sea level. This ratio is about 1.2 in the momentum interval considered by this experiment. The total intensity of negative mesons in this momentum interval is therefore about 5.0 particles/cm^2 steradian hr. Since the upper limit for the intensity of negative pi mesons in the momentum interval 0.45-1.75 bev/c is

2.5×10^{-3} particles/cm^2 steradian hr, these particles amount to less than 0.05% of the total intensity of negative mesons in the same momentum interval.

Very little information is available concerning the intensity of fast pi mesons. An attempt to determine this intensity was made by Mylroi and Wilson (16). As in the present experiment, these authors investigated those events in which negatively charged particles of known momenta came to rest in absorbers whose thicknesses were less than the ionization range of mesons corresponding to the known momenta. The momenta of the particles were measured by means of the magnetic spectrometer (17) shown schematically in Figure VI (a). Particles passing through the apparatus were deflected by the fields of the two electromagnets M1 and M2. The momenta were determined by analysis of the hodoscope record showing which tubes of trays A, B, and C were fired. In order to further define the beam, additional counters D and E were placed between the pole faces. Hodoscope records were made of all events showing fivefold coincidence among trays A, B, and C and counters D and E. Only those events in which a single tube in each of the three counter trays was fired were used for momentum determinations.

After leaving the momentum spectrometer, the particles entered the range analyzer shown in Figure VI (b). The amount of lead traversed by each particle was roughly indicated by

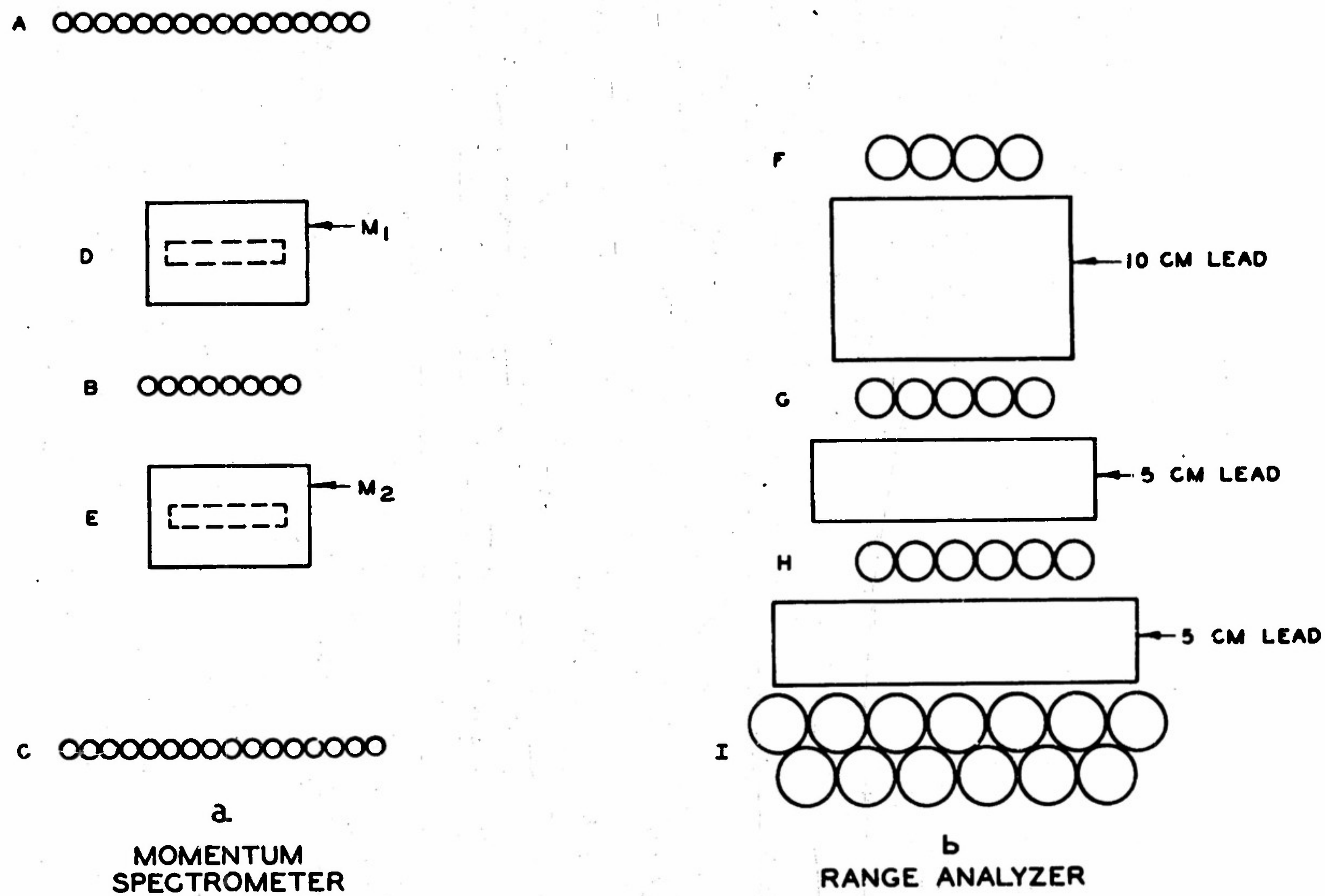

APPARATUS OF MYLROI AND WILSON

FIGURE VI

the firing or failure to fire of the counter trays below each absorber. Of 1974 negative particles passing through the apparatus, 4 were found to stop in 1-10 cm of lead, none in 10-15 cm, and 8 in 15-20 cm. Assuming that the particles were stopped by collisions with lead nuclei, a random process, the probability of a particle's stopping in the 5 cm of lead between trays G and H is just as great as the probability of its stopping in the 5 cm of lead between trays H and I. Therefore, it is the contention of the authors that the events indicating that 8 particles stopped in the last absorber can be ascribed to leakage of particles through counter tray I due to geometrical inefficiency and the dead time of the Geiger tubes. These 8 events were therefore ignored in the evaluation of an upper limit for the nuclear interaction of negative particles.

In order for a particle to be recorded as stopping in a particular absorber it must fail to trigger every tray of counters below that absorber. For this reason, the authors contend that the 4 events indicating that particles stopped in the first absorber are not due to counter inefficiency since the probability of trays G, H, and I all failing to be triggered by a particle passing through them is negligibly small. Furthermore, if the events indicating that particles were stopped in the first two absorbers were due to counter inefficiency, more events would be expected in the second absorber than in the first, since in this case only two trays need fail to fire instead of three. These four events must therefore be explained by means other than counter inefficiency.

Previous investigations with the spectrometer indicated that it gave spurious information in about 0.1% of the events. Therefore two of the stoppages observed during the experiment were attributed to this cause. The authors felt that the remaining two unexplained events might be due to fast electrons in spite of the strong biasing of the apparatus against these particles, or perhaps to the stopping of pi mesons by nuclear interactions in the lead. Therefore, by making allowances for an instrumental background that was as large or larger than the effect being sought, Mylroi and Wilson were able to set an upper limit of 0.1% on the fraction of energetic negative particles that are stopped in 10 cm of lead. This 0.1% is a raw instrumental figure. Computing from this an upper limit for the intensity of pi mesons in the atmosphere as was done for the present experiment, one finds that negative pi mesons make up less than 0.2% of the negative particles passing through the equipment. The present experiment places this upper limit at the smaller figure 0.05%. It is important to note that the upper limit set by the present experiment does not depend on any corrections for experimental error while that set by Mylroi and Wilson was found after attributing 6 out of 8 recorded events to spurious data.

C. Local Production of Mu Mesons

Since mu mesons are primarily produced by the decay of pi mesons, the upper limit for the intensity of pi mesons in the momentum interval considered by this experiment can be used to set an upper limit on the rate of local production of mu mesons in a corresponding momentum interval. The fraction of pi mesons with velocity β (in units of the velocity of light) which decay in a time interval t is given by $f = 1 - e^{-t/\tau_0 \gamma}$, where τ_0 is the proper mean life and γ is the Lorentz time dilation factor $(1-\beta^2)^{-1/2}$. The term f can be expressed as the fraction of pi mesons decaying in a path length x, and is given by $f = 1 - e^{-x/\gamma\beta\tau_0 c}$, where c is the velocity of light. The term $\gamma\beta$ is the momentum of the pi meson in units of $m_\pi c$ and, for the momentum interval 0.45-1.75 bev/c, has a mean value of about 8. Since τ_0 is about 2.5 X 10^{-8} seconds (18), the fraction of pi mesons in the stated momentum interval that decay in a distance of one meter is about 0.016. Since the results of this experiment show that the intensity of negative pi mesons in this momentum interval is less than 2.5 X 10^{-3} particles/cm^2 steradian hr, the rate of decay of these mesons is less than 4.0 X 10^{-5} particles/cm^2 sterad hr meter.

Because of the random angular distribution of mu mesons in the center of mass system, the mu mesons lie in a wider momentum interval than do the pi mesons producing them.

In order to set an upper limit for the production of mu mesons in a particular momentum interval, we must define that interval in such a way that only those pi mesons within the momentum interval 0.45-1.45 bev/c can contribute mesons to it.

From the conservation of energy and momentum, it can be shown (19) that the momentum of the decay mu meson must lie in the interval:

$$U_{\mu_0} P_{\pi} - P_{\mu_0} U_{\pi} < P_{\mu} < U_{\mu_0} P_{\pi} + P_{\mu_0} U_{\pi}$$

P_{π} and P_{μ} are the momenta of a pi meson and its decay mu meson expressed in "natural" units, i.e., in terms of $m_{\pi}c$ and $m_{\mu}c$. U_{π} is the energy of the pi meson in units of $m_{\pi}c^2$. U_{μ_0} and P_{μ_0} are the energy and momenta of a mu meson arising from the decay of a pi meson at rest.

Selecting the momentum limits under the requirements stated above, it is found that all mu mesons with momenta at the place of production that lie in the interval 0.45-1.02 bev/c were produced by the decay of pi mesons with momenta in the interval 0.45-1.75 bev/c.

Since the momentum distribution of pi mesons is not known, nothing can be said concerning the number of mu mesons with momenta outside the interval 0.45-1.02 bev/c which were produced by the decay of pi mesons with momenta in the interval 0.45-1.75 bev/c. However, the rate of pi meson decay in the momentum interval 0.45-1.75 bev/c can be taken as an upper limit for the production of mu mesons in the interval 0.45-1.02

bev/c. This conclusion depends upon the fact that for this momentum interval the direction of the mu meson in the laboratory system is very nearly that of the parent pi meson.

Summarizing, the rate of production at sea level of negative mu mesons in the momentum interval 0.45-1.02 bev/c is less than 4.0×10^{-5} particles/cm^2 sterad hr meter.

If one assumes that the positive to negative ratio for pi mesons in the momentum interval considered by this experiment is the same as the positive to negative ratio for mu mesons (which is not necessarily true), the total local production rate of mu mesons in the stated momentum interval would be less than 8.8×10^{-5} particles/cm^2 sterad hr meter.

D. <u>Removal Path Length of Mu Mesons</u>

The data discussed in Section B can be used to set a lower limit on the removal path length of mu mesons. From the flux density of negative mu mesons in the momentum interval 0.45-1.75 bev/c, and the effective admittance and operational time, it is found that about 4,700 negative mu mesons each passed through 147 g/cm^2 of material without any being stopped. The removal path length for mu mesons in this momentum interval is therefore greater than 6.9×10^5 g/cm^2. The corresponding upper limit for the removal cross section is 2.4×10^{-30} cm^2/nucleon. Since no particles were found to stop, no lower limit is imposed.

Several investigations of the nuclear interaction of fast mu mesons have been made in recent years (20 through 27). Most of these experiments have been conducted underground in order to reduce the number of events caused by nucleons and the electronic component. A summary of these experiments is given in Table II. Because of poor statistics and the diversity of event selection criteria, only rough agreement can be expected among them.

With the exception of the experiment by George and Evans, and that by Cocconi and Cocconi-Tongiorgi, the experiments listed in Table II detected the production of showers (principally pairs) of penetrating particles. Cocconi and Cocconi-Tongiorgi detected neutrons presumably produced by collisions of fast mu mesons in lead. The cross section given by George and Evans is based upon the production of stars with at least three heavily ionizing prongs in nuclear emulsions underground.

In all of these experiments there was no certainty that the events detected were actually produced by mu mesons. It is likely that at least some of them were produced by pi mesons and protons in equilibrium with the mu meson flux. The reported cross sections can, however, be taken as upper limits of the cross sections for the production of the particular type of event detected in each experiment.

TABLE II

NUCLEAR INTERACTION CROSS SECTION OF MU MESONS

Author	Method	Energy of Incident Particle in ev	Cross Section in 10^{-30} cm^2/nucleon
Amaldi et al	counters	10^{10}	13 ± 3
Amaldi and Fidecaro	counters	$(.2-.32) \times 10^9$ $>.3 \times 10^9$	45 23
Barret et al	counters	$.3 \times 10^{11}$	40 ± 20
Braddick et al	cloud chamber	6×10^9	50
Cocconi and C. Tongiorgi	BF_3 counters	5×10^9	9
George and Evans	emulsion	5×10^9 8×10^9 12×10^9	4.2 ± 0.7 4.5 ± 1.2 5.3 ± 1.7
George and Trent	counters	1.5×10^{10}	50
Lovati et al	cloud chamber	4×10^{10}	40
		Momentum of Incident Particle	Removal Cross Section in cm^2/nucleon
This Experiment	absorption in lead	0.45-1.75 bev/c	2.4×10^{-30}

The present experiment is more direct in the sense that there is no question that mu mesons traversed the equipment without being absorbed, and that no corrections had to be made for instrumental errors or for the nuclear collisions of pi mesons, protons, or other particles. The experiment is, however, subject to the criticism that there is an ambiguity in the relationship between the removal cross section and the cross section for nuclear interaction. The work of Garrison has shown that for protons in the momentum interval considered in this experiment there is no significant difference between the two cross sections. There is no reason to feel, however, that this is the case for nuclear collisions of mu mesons.

E. Apparent Anomalous Absorption at 3.4 Km

It is of interest to compare the rates of apparent anomalous absorption of negative particles observed in previous experiments by this laboratory with the expected rate of leakage of particles through the anti-coincidence tray due to counter dead time.

In 1950 Todd (9) conducted an experiment at sea level in which the momentum spectrum was determined for those particles which apparently stopped in 10 cm of lead. The anti-coincidence tray used in that experiment was made of glass walled Geiger tubes so arranged that most particles which traversed the lead absorber passed through only one tube. The counting rate of single anti-coincidence tubes was about 4.0 counts per second. Since the recovery time was about 500 microseconds the tubes were insensitive for about 0.2% of the operational time. That is, about 0.2% of the particles passing through the anti-coincidence tray should fail to trigger any tube. This calculated leakage rate is to be compared with the observed rate of apparent anomalous absorption. In the momentum interval 1-2 bev/c (well beyond the ionization cutoff) the observed rate of negative particles that apparently stopped in the absorber was 0.011 ± 0.005 particles/cm^2 steradian hr, the indicated error being the standard deviation. Integrating Rossi's momentum spectrum over the same momentum interval and assuming that the sea level positive-negative ratio for mu mesons is 1.2, one finds that the total intensity of negative mu mesons within this momentum interval is 3.1 particles/cm^2 steradian hr. The observed absorption rate is therefore $(.4 \pm .2)$% of the intensity of negative mesons. The accuracy of both the estimated and the observed leakage rates is poor, but it is seen that counter inefficiency due to dead time could have accounted for the observed anomalous absorption at sea level. By removing this source of error, the present experiment demonstrates beyond a doubt that the observed apparent absorption was indeed due to counter inefficiency.

In 1950 Garrison determined the momentum spectrum of those particles absorbed in 15 cm of lead at an altitude of

3.4 km (1). The results of this experiment have been shown in Figure I. In the following year Sandstrom (12) also found the momentum spectrum of particles absorbed in 15 cm of lead at this altitude. The results of these two experiments agree within the statistical accuracy and are treated together in the following discussion.

In the experiments of Garrison and Sandstrom the anti-coincidence tray was made up of copper walled tubes so arranged that most particles traversing the lead absorber had to pass through two Geiger tubes. Consequently a particle could not pass through the tray without triggering a counter unless both counters through which it passed had been previously discharged within a period of about 500 microseconds. By estimating the coincidence counting rate of two adjacent tubes at 3.4 km, it is found that leakage due to counter dead time is less than 0.2%.

This predicted value of the leakage of the anti-coincidence tray is now to be compared with the observed intensity of anomalous absorption of negative particles in the momentum interval 1-2 bev/c. Garrison obtained an intensity in this momentum interval of 0.12 ± 0.02 particles/cm^2 steradian hr, while Sandstrom found 0.16 ± 0.05 particles/cm^2 steradian hr. Combining the results of these experiments and comparing them with the total intensity as found by Potter (2) at the same altitude, it is found that the observed anomalous absorption of negative particles at 3.4 km amounts to (2.5 ± .4)% of the total negative meson component in the momentum interval considered. Comparing this with the expected leakage rate (less than 0.2%), it is evident that counter inefficiency does not account for the anomalous absorption of negative particles observed in these experiments.

This result indicates that there may be a measurable intensity of pi mesons or of one or more of the other types of particles and events as listed in Section A at 3.4 km. No such measurable intensity was found at sea level in the present experiment. Quantitatively, such anomalous absorption at 3.4 km may be 100 times greater than the upper limit set at sea level. As this is a positive result the problem of errors of inclusion becomes a critical one, in contrast to the present experiment in which no anomalous absorption was detected. The experimental arrangement does not give assurance against errors of inclusion due to back scattering. One such event occurred in the present experiment which fortunately could be identified by the ionization density and radius of curvature of the cloud chamber track. Examination of the apprently anomalously absorbed particles in the experiments of Garrison and Sandstrom shows most of them to be of high momentum and minimum ionization, so they cannot be identified. Little more can be said at present concerning the apparent anomalous absorption at 3.4 km. It would seem worth while to conduct an experiment of the type described in this thesis at higher altitudes, but provision should be made for greater protection against back scattered particles.

CHAPTER V

SUMMARY

The principal result of this experiment is contained in the statement that at sea level the intensity of negative non-electronic particles in the momentum interval 0.37-1.67 bev/c that are absorbed in 147 g/cm^2 of lead is less than 1.0 X 10^{-3} particles/cm^2 steradian hr. This result has been used to set an upper limit of 2.5 X 10^{-3} particles/cm^2 steradian hr on the intensity of negative pi mesons in the momentum interval 0.45-1.75 bev/c. This upper limit corresponds to 0.05% of the total negative meson intensity in this momentum interval. The same upper limit has been set for the intensity of negative protons in the momentum interval 0.69-1.75 bev/c. A lower limit of 6.9 X 10^5 g/cm^2 or 6.1 X 10^4 cm of lead has been set on the removal path length of mu mesons in the momentum interval 0.37-1.67 bev/c. It has been shown that the local production of mu mesons in the momentum interval 0.45-1.02 bev/c is less than 8.8 X 10^{-5} particles/cm^2 steradian hr meter. It has been pointed out that there may be a measurable intensity of anomalous absorption of negative particles at an altitude of 3.4 km. The momentum spectrum has been obtained for those non-electronic particles that stop in 10 cm of lead at sea level. This spectrum is a confirmation of the principal aspects of the spectrum obtained by Todd at sea level.

BIBLIOGRAPHY

1. G. Garrison. Ph.D. thesis, University of Washington, 1952
2. D. S. Potter, Ph.D. thesis, University of Washington, 1951
3. F. M. Charbonnier. Ph.D. thesis, University of Washington, 1952
4. R. A. Montgomery. Phys. Rev. 75:1407 (1949)
5. J. C. Street and R. H. Woodward. Phys. Rev. 46:1029 (1934)
6. G. D. Rochester and C. C. Butler. Nature 160:855 (1947)
7. A. J. Seriff, R. B. Leighton, C. Hsiao, E. W. Cowan and C. D. Anderson. Phys. Rev. 78:290 (1950)
8. H. S. Bridge and M. Annis. Phys. Rev. 82:445 (1951)
9. Jay Todd, Jr. Ph.D. thesis, University of Washington, 1952
10. C. E. Miller, J. E. Henderson, D. S. Potter and Jay Todd, Jr. Phys. Rev. 79:459 (1950)
11. C. E. Miller, J. E. Henderson, D. S. Potter, and Jay Todd, Jr. Phys. Rev. 84:981 (1951)
12. W. M. Sandstrom. Ph.D. thesis, University of Washington, 1953
13. J. G. Wilson. Progress in Cosmic Ray Physics, International Publishers Inc., New York, 1952
14. V. Camerini, P. H. Fowler, W. O. Lock and H. Muirhead. Phil. Mag., 41:413 (1950); Phil. Mag. 43:1241 (1951)
15. B. Rossi, Rev. Mod. Phys. 20:537 (1948)
16. M. G. Mylroi and J. G. Wilson. Proc. Phys. Soc. A 64:404 (1951)
17. B. D. Hyams, M. G. Mylroi, B. G. Owen and J. G. Wilson. Proc. Phys. Soc. A 63:1053
18. W. L. Kraushaar. Phys. Rev. 86:513 (1952)

19. G. Ascoli. Phys. Rev. 79:812 (1950)

20. E. Amaldi, C. Castagnoli, A. Gigli and S. Sciuti. Nuovo Cimento 9:969 (1952)

21. E. Amaldi and G. Fidecaro. Phys. Rev. 81:339 (1951)

22. P. H. Barrett, L. M. Bollinger, G. Cocconi, Y. Eisenberg and K. Greisen. Rev. Mod. Phys. 24:133 (1952)

23. H. J. J. Braddick, W. F. Nash and A. W. Wolfendale. Phil. Mag. 42:1277 (1951)

24. G. Cocconi and V. Cocconi-Tongiorgi. Phys. Rev. 84:29 (1951)

25. E. P. George and J. Evans. Proc. Phys. Soc. A 63:1248 (1950)

26. E. P. George and P. T. Trent. Proc. Phys. Soc. A 64:1134 (1951)

27. A. Lovati, A. Mura, C. Succi and G. Tagliaferri. Nuovo Cimento X:105 (1953)

28. K. J. Le Couteur. Proc. Phys. Soc. A 63:259 (1950)